Measurements of Low Optical Power with Cryostat-Based Predictable Quantum Efficient Detector at Liquid Nitrogen Temperature

Mikhail Korpusenko[1], Meelis-Mait Sildoja[2,3], Farshid Manoocheri[1], and Erkki Ikonen[1,4]

[1]Metrology Research Institute, Aalto University, Espoo, Finland; [2]METROSERT, Tallinn, Estonia; [3]National Institute of Chemical Physics and Biophysics, Tallinn, Estonia; [4]VTT MIKES, Espoo, Finland
Corresponding e-mail mikhail.korpusenko@aalto.fi

We have validated optical power measurements with a Predictable Quantum Efficient Detector (PQED) at liquid nitrogen temperature (77 K) at low optical power from 130 fW to 3.3 pW. Two laser wavelengths at 514 nm and 785 nm were used. The lowest measured optical power corresponds to a photon flux of $0.5 \cdot 10^6$ photons per second (785 nm). The PQED's responsivity is linear within the relative measurement uncertainties of 8% at $0.5 \cdot 10^6$ ph/s and 1.4% at $10 \cdot 10^6$ ph/s (95% confidence level), which enables the calibration of other low photon flux detectors directly against a primary standard of optical power.

1. Introduction

Accurate single photon measurements are in high demand in quantum applications. Photon counting is essentially required for quantum computing [1,2], cryptography [3,4], low-intensity bio-microscopy [5], and quantum key distribution [6]. Widely used Single Photon Avalanche Photodiode (SPAD) and detector arrays based on that are commonly used to measure optical flux from millions to hundreds of photons per second [7]. Principally, there are three approaches for such calibration. It can be comparison measurement against calibrated detector [8–14], source-based calibration [15], or a self-calibration technique [16–18]. Calibration of SPADs is a challenging task since such single photon detectors cannot be calibrated directly against Absolute Cryogenic Radiometer (ACR) [19–22] due to insufficient sensitivity of the latter at such low optical fluxes. This limitation requires to execute several traceable measurements for SPAD calibration which is demanding in terms of calibration time and maintenance service of calibration facility. Several traceable measurements affect calibration uncertainty as well.

Another approach is to apply self-calibration techniques which can be based on photon-statistics of a nonlinear source [17], squeezed vacuum state of a source [16], or time correlation of entangled photons pairs [18]. These techniques yield "absolute" calibration without reference detector and thus traceability to SI which is a strong benefit itself. At this moment, National Metrology Institutes (NMIs) cannot provide absolute calibrations with self-calibration methods according to the BIPM Mise en pratique for the definition of the candela as mentioned in appendix 2 of the SI Brochure, 9th edition (2019) [23].

Two kinds of detectors may act as primary optical standard. ACR is a thermal detector cooled to cryogenic temperature (< ~20 K). Only limited number of NMIs maintain ACR for absolute calibrations due to its high purchase cost. In order to provide more convenient calibration capabilities, NMI community has developed a novel detector which is also acknowledged as primary optical standard [23]. Predictable Quantum Efficient Detector (PQED) [24,25] is a

wedge trap detector based on two induced-junction Si photodiodes. Very low reflectance [26], recombination losses [27], and spatial non-uniformity of tens of parts per million (ppm) provide predictable responsivity of PQED over visible range which makes it a suitable candidate for responsivity calibration at low optical power [28]. To overcome the sensitivity limit of room temperature PQED, the detector can be cooled to decrease the dark current and its fluctuations.

In this work we executed measurements with the cryostat-based n-type PQED [29] at liquid nitrogen temperature (77 K) at power levels from 130 fW to 3.3 pW in the visible range to study its applicability as a reference detector. This photodector with predictable responsivity at very low incident optical flux can be used for calibration of single photon detectors, avalanche photodiodes and other low-flux detectors. In addition, we conducted a calibration measurement of another low photon flux detector based on cooled pn-junction photodiode by Hamamatsu. We aim to simplify the calibration procedure and shorten the traceability chain to a primary optical power standard, i.e, to the PQED.

2. Studied detectors

2.1 Cryostat based PQED

PQED is designed to convert every absorbed photon to an electron-hole pair without recombination losses. The detector thus ideally produces a photocurrent with the spectral responsivity of $R(\lambda) = e\lambda/hc$ depending only on fundamental constants and vacuum wavelength λ. The real responsivity is based on simulation with a 3D model of charge carrier recombination losses, which can predict internal losses at the uncertainty level of a few tens of ppm (parts per million) [30]. The responsivity of PQEDs made of p-type photodiodes has been confirmed to follow the ideal equation $R(\lambda) = e\lambda/hc$ within 100 ppm in comprehensive comparison measurements against cryogenic radiometers [31]. Furthermore, the responsivity changes are small when cooling the PQED from room temperature to 77 K.

Previous studies of the n-type PQED at room temperature showed internal losses at a level of 170 ppm at 532 nm [32] and at 785 nm a small increase of internal losses has been observed [33]. However, the dark current at room temperature is smaller for *n*-type PQED photodiodes than for p-type photodiodes, difference is at a level of several nA [28,32]. The dark current of biased n-type PQED photodiodes can be reduced by several orders of magnitude to pA level when cooling from room temperature to liquid nitrogen temperature [28].

The detector is based on a PQED made of n-type photodiodes inside a liquid nitrogen temperature cryostat (Figure 1). The cryostat is pumped with a combination of a scroll pump and a turbomolecular pump. A radiation shield with 10 mm input aperture is connected directly to the liquid nitrogen (LN) vessel. The radiation shield encloses the photodiodes and serves as a cold trap. The photodiode holder is in a copper-to-copper thermal connection with the LN vessel. The cryostat also contains a charcoal getter to trap permeated gases. A flat

glass window calibrated against room temperature PQED serves as an entrance window and ensures airtight connection.

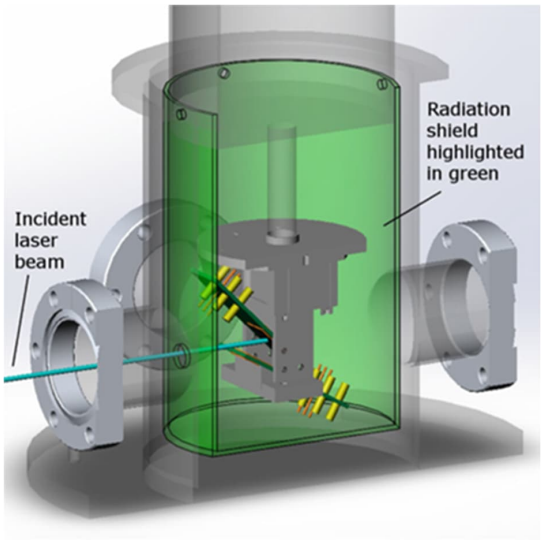

Figure 1. Schematic drawing of the cryostat. The radiation shield has an aperture 10 mm in diameter for the incident laser beam to reach the wedge-arranged photodiodes [29].

2.2 Low photon flux detector

We used the PQED to calibrate a cooled, low flux photon detector from the National Institute of Chemical Physics and Biophysics (KBFI). The detector is used in several applications of weak fluorescence measurements and non-linear spontaneous parametric down conversion experiments. The detector consists of a commercial Hamamatsu photodiode S1337 with active area of 5 mm x 5 mm and in-house built switched integrator amplifier (SIA) based on IVC102 chip from Texas Instruments. The working principle of the integrator-based amplifier can be found elsewhere [34]. In this case the amplifier is controlled by National Instruments DAQ board NI USB-6210 using dedicated LabView software. The photodiode is housed in a small cryostat similar to dewars provided by Infrared Associates and is cooled to liquid nitrogen temperature. The illumination of the photodiode is through a quartz window.

3. Measurement setup

We performed optical power measurements of the cryostat-based PQED at LN temperature in the range 130 fW to 3.3 pW at air wavelengths of 514.5 nm (Ar^+ laser) and 784.82 nm (single mode semiconductor laser) with p polarized light (Figure 2). Low optical flux of several millions of photons per second is achieved by attenuation of the incident laser beam of 2.4 mm in diameter ($1/e^2$) with calibrated high optical density filters. We used two sets of absorptive filters with antireflection coating to reduce light scattering. These filters were slightly tilted to avoid interreflections. In addition, we used narrow bandwidth filters for each

wavelength to isolate the PQED from heterochromatic stray light, baffle sheets, and tubes to minimize scattered light reaching PQED. With these precautions, dark levels of the current of the cooled PQED with closed and open inner all metal gate valve were similar when the lasers were off. Keysight B2985 electrometer served as the photocurrent measurement device. The integration time of one reading was 2 seconds, and one measurement round contains 30 photocurrent data readings followed by 30 dark current readings and another 30 readings followed by 30 dark current readings. Dark current readings were obtained with closed shutter.

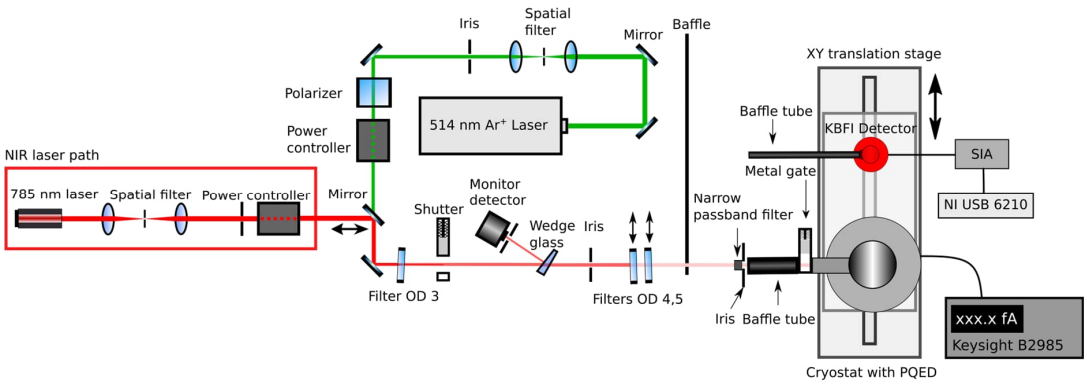

Figure 2. Measurement setup for low flux measurements. Only one laser was used at a time.

The setup of Figure 2 was also used to calibrate the KBFI detector described in Sec. 2.2. Measurements with the PQED determine the low optical power of the laser beam. Using the XY translation stage the detectors are interchanged in front of the laser beam and the response of the KBFI detector is recorded at the nominal position of the PQED.

4. Measurement results

4.1 Linearity measurement

The full optical power of the laser beam was first measured by the PQED without any attenuation by the filters. A calibrated transimpedance amplifier and sufficient reverse bias voltage were used for this measurement. Then cascaded filters of known transmittance were inserted in the beam path to reduce the optical power to the desired range. Low photocurrent I_{meas} of the PQED was measured with Keysight B2985 electrometer and divided by the expected photocurrent I_{calc} obtained on the basis of the known filter attenuation of the full optical power. The measurement results at two different wavelengths are shown in Figure 3.

The relative standard uncertainty of 0.35% of I_{calc} is determined by measurements of filter attenuation and unattenuated optical power of the laser beam. The transmittance of each antireflection-coated neutral density filter was measured separately by PQED with calibrated

transimpedance amplifier. After calibration measurement, filters were not taken off from the flip stages and not moved laterally or angularly during actual measurement. For several subsequent measurements of I_{meas}, the average photocurrent and dark current were stable within a standard deviation of approximately 5 fA. After moving the PQED with XY translation stage, the average dark current varied between 30 fA and 60 fA depending on cable bending and tension. The signal current I_{meas} was calculated as a difference of photocurrent and dark current cancelling electrical and straylight biases. The uncertainty bars in Figure 3 are mainly caused by repeatability of measurements and electrometer uncertainty. It is seen that PQED's responsivity is linear well within the expanded uncertainty.

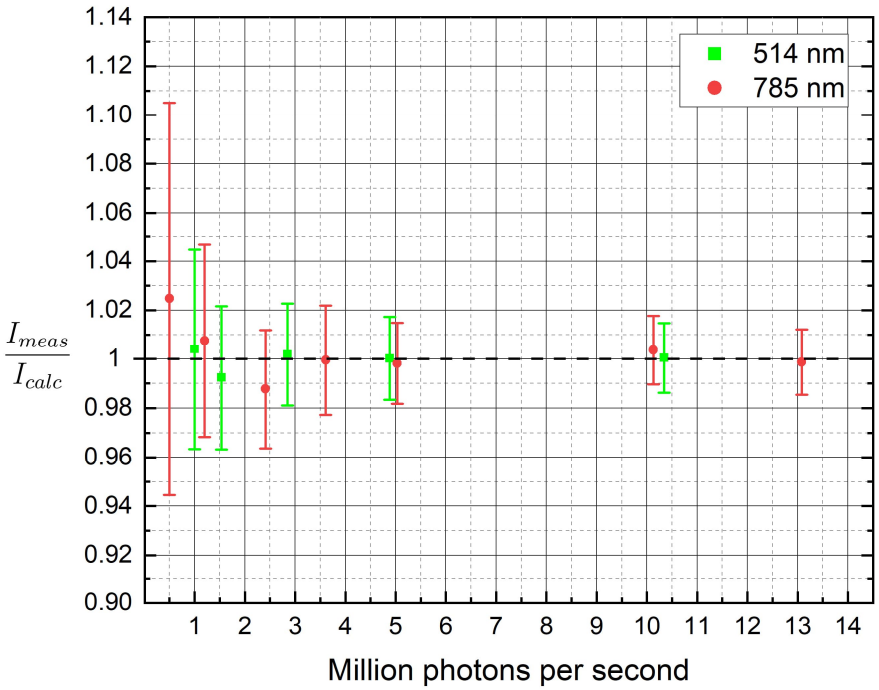

Figure 3. Ratio of measured and expected photocurrent at different photon flux levels corresponding to optical power range from 130 fW to 3.3 pW. The error bars are given at 95% confidence level.

4.2 KBFI detector calibration

Calibration measurement of the KBFI detector was carried out at the wavelength of 785 nm and in the photon flux range from 0.5 to 10 million photons per second (ph/s). We used Edmund Optics 39-334 passband filter with transmission of 99% at 785 nm. Such a transmission allows to significantly diminish interreflections between the filter and the photodiode of 30% reflectance. Baffles of the detectors were moved tightly to the passband filter and iris behind it to prevent straylight incidence. The amplifier was separately calibrated against current-source Keithley 263 calibrated by VTT MIKES at nominal current level of 1 pA.

An example of uncertainty budgets for optical power measurement with the PQED is shown in Table 1 at the photon rate of 0.5 million ph/s corresponding to a signal current of 75 fA. A

significant uncertainty component is related to repeatability of photocurrent measurements where the standard deviation of the mean is 1.8 fA after repositioning the PQED and KBFI detector three times with the XY translation stage. Repeatability is affected by fluctuations in photocurrent and dark current. This component also includes straylight variations and any other sources of electrical noise or leakage current. Specifications of Keysight B2985 electrometer give an accuracy of ±(1% + 3 fA) in the used measurement range. This value is assumed to describe the limits of uniform probability distribution from which the standard uncertainty is calculated by dividing it with $\sqrt{3}$.

For the remaining relative uncertainty components in Table 1, window transmittance and its uncertainty are obtained from a comparison measurement against a similar room temperature PQED. The responsivity of the n-type PQED has been determined earlier [32]. Spatial responsivity of the cryostat-based PQED was studied at room temperature before assembling the flat glass window. The expanded uncertainty is calculated using the coverage factor $k = 2.16$ obtained from the effective degrees of freedom (DoF) for 95% confidence level. Similarly to Table 1, the combined relative standard uncertainty and expanded uncertainty are calculated separately at each photon rate.

Table 1. Uncertainty budget for low optical power measurements with cooled cryostat-based PQED. DoF denotes degrees of freedom.

		0.5 million ph/s	
Uncertainty component	DoF	Absolute uncertainty (fA)	Relative uncertainty (%)
Repeatability ($n = 3$)	2	1.8	2.3
Current measurement	∞	2.2	2.9
Window transmittance	∞	0.01	0.01
PQED responsivity	∞	0.01	0.01
PQED spatial responsivity	∞	0.002	0.003
Combined relative standard uncertainty	13		3.7

The calibration results of KBFI detector are shown in Table 2. Nominal responsivity of the S1337 photodiode is used to record the signal of the KBFI detector. The dominant uncertainty contribution of the KBFI detector depends on the measured photon flux level: for the two lowest photon flux levels, the dominant contribution is measurement noise, while the major contributors at larger photon rates are the uncertainty of calibration of the amplifier and the uncertainty due to losses on optical surfaces.

Tabie 2. Results of PQED and KBFI detectors measuring several photon flux levels between 0.5 million ph/s and 10 million ph/s. The measured photon rate of KBFI detector is based on nominal responsivity of the photodiode.

Measured photon rate with PQED, million ph/s	Uncertainty of PQED, 95% confidence level	Measured photon rate of KBFI detector, million ph/s	Uncertainty of KBFI detector, 95% confidence level	Correction factor KBFI detector / PQED
0.50	8.0%	0.49	5.0%	0.984
1.20	3.9%	1.18	3.7%	0.983
2.41	2.4%	2.40	1.6%	0.997
5.03	1.7%	5.02	1.5%	0.999
10.13	1.4%	10.02	1.5%	0.989

5. Conclusions

We performed a linearity measurement of liquid nitrogen cooled n-type PQED over the power level from $1.3 \cdot 10^{-13}$ W to $3.3 \cdot 10^{-12}$ W at two laser wavelengths of 514 nm and 785 nm. Results showed that cryostat-based PQED is linear within the measurement uncertainty. In addition, a calibration measurement of dedicated low optical flux detector from KBFI at five power levels was carried out at the wavelength of 785 nm. The calibration results were compared with the nominal responsivity of the KBFI detector, indicating that both detectors agree well within the measurement uncertainties, which are approximately 8.0% at 0.5 million photons/s and 1.4% at 10.13 million photons/s for the PQED at the 95% level of confidence.

At this stage, ripple and drift of the PQED signal and dark current are the main uncertainty components which can be potentially reduced by improving electrical cabling and grounding and by suppressing further the straylight, e.g by installing light tight box around the PQED detector. In overall, LN cooled PQED shows good potential to be a reference detector for responsivity calibrations at low optical powers of 130 fW and above.

Acknowledgments

This work was funded by the project SEQUME (contract 20FUN05) of the European Metrology Programme for Innovation and Research (EMPIR). The EMPIR is jointly funded by the EMPIR participating countries within EURAMET and the European Union's Horizon 2020 Programme. The work is part of the Research Council of Finland Flagship Programme, Photonics Research and Innovation (PREIN), decision number 346529, Aalto University.

Reference list

[1] Ceccarelli F, Acconcia G, Gulinatti A, Ghioni M, Rech I and Osellame R 2021 Recent Advances and Future Perspectives of Single-Photon Avalanche Diodes for Quantum Photonics Applications *Adv Quantum Technol* 4 2000102

[2] Hadfield R H 2009 Single-photon detectors for optical quantum information applications *Nat Photonics* 3 696–705

[3] Jain N, Anisimova E, Khan I, Makarov V, Marquardt C and Leuchs G 2014 Trojan-horse attacks threaten the security of practical quantum cryptography *New J Phys* 16 123030

[4] Townsend P D 1998 Experimental investigation of the performance limits for first telecommunications-window quantum cryptography systems *IEEE Photonics Technology Letters* 10 1048–50

[5] Bruschini C, Homulle H, Antolovic I M, Burri S and Charbon E 2019 Single-photon avalanche diode imagers in biophotonics: review and outlook *Light Sci Appl* 8 1–28

[6] Zhang J, Eraerds P, Walenta N, Barreiro C, Thew R and Zbinden H 2010 2.23 GHz gating InGaAs/InP single-photon avalanche diode for quantum key distribution *Proc. SPIE 7681, Advanced Photon Counting Techniques IV* ed M A Itzler and J C Campbell pp 1–8

[7] Chunnilall C J, Degiovanni I Pietro, Kück S, Müller I and Sinclair A G 2014 Metrology of single-photon sources and detectors: a review *Optical Engineering* 53 081910

[8] Brida G, Genovese M, Gramegna M, Rastello M L, Chekhova M and Krivitsky L 2005 Single-photon detector calibration by means of conditional polarization rotation *Journal of the Optical Society of America B* 22 488–92

[9] López M, Hofer H and Kück S 2015 Detection efficiency calibration of single-photon silicon avalanche photodiodes traceable using double attenuator technique *J Mod Opt* 62 1732–8

[10] Lee H J, Park S, Park H S, Hong K S, Lee D-H, Kim H, Cha M and Moon H S 2016 Wavelength-scanning calibration of detection efficiency of single photon detectors by direct comparison with a photodiode *Metrologia* 53 908–17

[11] Müller I, Klein R M and Werner L 2014 Traceable calibration of a fibre-coupled superconducting nano-wire single photon detector using characterized synchrotron radiation *Metrologia* 51 S329–35

[12] Gerrits T, Migdall A, Bienfang J C, Lehman J, Nam S W, Splett J, Vayshenker I and Wang J 2020 Calibration of free-space and fiber-coupled single-photon detectors * *Metrologia* 57 1–18

[13] Lunghi T, Korzh B, Sanguinetti B and Zbinden H 2014 Absolute calibration of fiber-coupled single-photon detector *Opt Express* 22 18078–92

[14] Vaigu A, Porrovecchio G, Chu X-L, Lindner S, Smid M, Manninen A, Becher C, Sandoghdar V, Götzinger S and Ikonen E 2017 Experimental demonstration of a predictable single photon source with variable photon flux *Metrologia* 54 218–23

[15] Georgieva H, López M, Hofer H, Kanold N, Kaganskiy A, Rodt S, Reitzenstein S and Kück S 2021 Absolute calibration of a single-photon avalanche detector using a bright triggered single-photon source based on an InGaAs quantum dot *Opt Express* 29 23500–7

[16] Mogilevtsev D 2010 Calibration of single-photon detectors using quantum statistics *Phys Rev A (Coll Park)* 82 021807

[17] Cohen L, Pilnyak Y, Istrati D, Studer N M, Dowling J P and Eisenberg H S 2018 Absolute calibration of single-photon and multiplexed photon-number-resolving detectors *Phys Rev A (Coll Park)* 98 013811

[18] Chen X-H, Zhai Y-H, Zhang D and Wu L-A 2006 Absolute self-calibration of the quantum efficiency of single-photon detectors *Opt Lett* 31 2441

[19] Martin J E, Fox N P and Key P J 1985 A Cryogenic Radiometer for Absolute Radiometric Measurements *Metrologia* 21 147–55

[20] Varpula T, Seppa H and Saari J-M 1989 Optical power calibrator based on a stabilized green He-Ne laser and a cryogenic absolute radiometer *IEEE Trans Instrum Meas* 38 558–64

[21] Foukal P V., Hoyt C, Kochling H and Miller P 1990 Cryogenic absolute radiometers as laboratory irradiance standards, remote sensing detectors, and pyroheliometers *Appl Opt* 29 988

[22] Datla R U, Stock K, Parr A C, Hoyt C C, Miller P J and Foukal P V. 1992 Characterization of an absolute cryogenic radiometer as a standard detector for radiant-power measurements *Appl Opt* 31 7219

[23] Zwinkels J, Sperling A, Goodman T, Acosta J C, Ohno Y, Rastello M L, Stock M and Woolliams E 2016 Mise en pratique for the definition of the candela and associated derived units for photometric and radiometric quantities in the International System of Units (SI) *Metrologia* 53 G1–G1

[24] Sildoja M, Manoocheri F, Merimaa M, Ikonen E, Müller I, Werner L, Gran J, Kübarsepp T, Smîd M and Rastello M L 2013 Predictable quantum efficient detector: I. Photodiodes and predicted responsivity *Metrologia* 50 385–94

[25] Müller I, Johannsen U, Linke U, Socaciu-Siebert L, Smîd M, Porrovecchio G, Sildoja M, Manoocheri F, Ikonen E, Gran J, Kübarsepp T, Brida G and Werner L 2013 Predictable quantum efficient detector: II. Characterization and confirmed responsivity *Metrologia* 50 395–401

[26] Sildoja M, Manoocheri F and Ikonen E 2009 Reflectance calculations for a predictable quantum efficient detector *Metrologia* 46 S151–4

[27] Dönsberg T, Sildoja M, Manoocheri F, Merimaa M, Petroff L and Ikonen E 2014 A primary standard of optical power based on induced-junction silicon photodiodes operated at room temperature *Metrologia* 51 197–202

[28] Porrasmaa S, Dönsberg T, Manoocheri F and Ikonen E 2020 Predictable quantum efficient detector for low optical flux measurements *Opt Rev* 27 190–4

[29] Manoocheri F, Dönsberg T, Sildoja M, Smíd M, Porrovecchio G and Ikonen E 2018 Liquid nitrogen cryostat for predictable quantum efficient detectors *J Phys Conf Ser* 972 012021

[30] Tran T, Porrovecchio G, Smid M, Ikonen E, Dönsberg T and Gran J 2022 Determination of the responsivity of a predictable quantum efficient detector over a wide spectral range based on a 3D model of charge carrier recombination losses *Metrologia* 59 045012

[31] Porrovecchio G, Linke U, Smid M, Gran J, Ikonen E and Werner L 2022 Long-term spectral responsivity stability of predictable quantum efficient detectors *Metrologia* 59 065008

[32] Dönsberg T, Manoocheri F, Sildoja M, Juntunen M, Savin H, Tuovinen E, Ronkainen H, Prunnila M, Merimaa M, Tang C K, Gran J, Müller I, Werner L, Rougié B, Pons A, Smîd M, Gál P, Lolli L, Brida G, Rastello M L and Ikonen E 2017 Predictable quantum efficient detector based on *n* -type silicon photodiodes *Metrologia* 54 821–36

[33] Korpusenko M, Manoocheri F, Kilpi O-P, Varpula A, Kainlauri M, Vehmas T, Prunnila M and Ikonen E 2022 Characterization of predictable quantum efficient detector at 488 nm and 785 nm wavelengths with an order of magnitude change of incident optical power *Meas Sci Technol* 33 015206

[34] Mountford J, Porrovecchio G, Smid M and Smid R 2008 Development of a switched integrator amplifier for high-accuracy optical measurements *Appl Opt* 47 5821